



Determination of Natural Radioactivity Concentration and Radiogenic Heat Production in Selected Quarry Sites in Ondo State, Nigeria

Asere, Adeola Margaret* and Sedara, Samuel Omosule

Department of Physics and Electronics, Adekunle Ajasin University, Akungba-Akoko, Ondo State

*Email: adeola.asere@aaua.edu.ng ^bEmail: samuel.sedara@aaua.edu.ng

Article Info

Received 26 July 2020

Revised 03 August 2020

Accepted 07 August 2020

Available online 31 August 2020

Keywords:

natural radioactivity, activity concentration, granite, radiogenic heat production, radiological parameters



<https://doi.org/10.37933/nipes/2.3.2020.26>

<https://nipesjournals.org.ng>

© 2020 NIPES Pub. All rights reserved

Abstract

Gamma-ray spectrometer was used to measure radiation from radio-nuclides inside and outside five different quarry sites in Ondo State (Sutol, Batista, Aslos, Johnson and Stoneworks) in order to determine the pattern of natural radioactivity, radiogenic heat production effect and radiological health risk to the population within the site vicinity. The average activity concentration of ^{238}U , ^{232}Th and ^{40}K inside the quarries are 47.09 ± 7.49 , 95.02 ± 14.11 and $1118.68 \pm 126.94 \text{ Bqkg}^{-1}$ and outside the quarries are 35.76 ± 7.83 , 83.17 ± 11.85 and $959.71 \pm 96.43 \text{ Bqkg}^{-1}$ consecutively. The total heat production and heat flow values estimated for all the quarries varied from 0.97 to $5.37 \mu\text{Wm}^{-3}$ and 7.63 to 42.12 mWm^{-2} respectively. The radiogenic heat production variations with the radionuclide from the quarries were presented as plots. Thorium concentration is highest (43.5 ppm) followed by uranium (10.4 ppm). The mean values of all the hazard indices calculated were lower than the internationally acceptable limits. This implies that, the people working in the quarries, granite end-users and general public living around the quarries area are safe from radiological health risk. Considering radiogenic and thermal modeling point of view, the Johnson quarry has the highest concentration of uranium, total heat production and heat flow values. It is a manifestation of the geological rock types and presence of highly weathered minerals. So, it is of most promising Uranium mineralization and further probe for potential geothermal exploration.

1. Introduction

Natural radioactivity, ^{238}U , ^{232}Th and ^{40}K decay series are relatively abundant in the natural environment. They are the only naturally produced gamma radiation of sufficient energy and intensity to be measured by gamma ray spectrometry [1]. This technique allows the calculation of the heat produced during radioactive decay of potassium, uranium, and thorium within rock. Radiogenic heat producing rocks are often targets for geothermal exploration and production. It has a wide range of applications beyond geothermal exploration including: uranium exploration [2], sedimentary facies identification for oil and gas exploration, detection of radioactive contamination and mineral exploration. It can also be used for pure earth science discoveries, e.g., constraining deep crustal processes from potassium, uranium, and thorium concentrations in

modern day outcrops [3, 4, 5]. Elevated concentration of these Naturally Occurring Radioactive Material (NORM) are often found in certain geological materials, especially certain igneous rocks and ores [6]. Human activities such as quarrying that exploit these natural radioactive materials could result in the enhanced potential for exposure to naturally occurring radioactive materials [7]. The presence of naturally occurring radionuclides mainly due to gamma radiation from ^{238}U , ^{232}Th and ^{40}K decay series which originate from granite quarrying offers radiation exposure both to workers in the quarry, people residing very close to the quarry, and buildings in which the granite would be used. Quarry products consist of different geological materials such as granite, gneiss, diorite, granodiorite, and other rocks that after an industrial process are suitable for use as building materials and ornamental rocks [8, 9]. Rocks of high concentrations of these radioelements can be characterized by high heat flow, and the geothermal gradient can thus be favourably enhanced. Such enhancement creates useable heat at shallower depths than would otherwise be the case, thus reducing the drilling costs of a geothermal project. Many granites are enriched in the radioelements potassium, thorium and uranium, and thus typically have higher radioactivity than many other rocks. Granite is therefore a favoured target in geothermal exploration worldwide [10]. Granite is a common type of felsic intrusive igneous rock which is granular and phaneritic in texture. Granite forms a major part of continental crust and has to be quarried before use due to its hard nature, being a rock. Granite can be crushed and used as crushed stones or used as an aggregate. It can be used in various applications when been cut into tiles and slabs such as tile floors, stair threads and countertops. It can be used in monuments, building, paving and bridges. Radiogenic heat production is not just a phenomenon peculiar to granite as all rocks contain some concentration of radioelements. Depending on the depositional environment, mudstones can have elevated concentrations of radioelements compared to other sedimentary rocks. Due to their low thermal conductivities (because of their low quartz content) this heat can remain in place within mudstones over geological time, which may result in viable geothermal resources. Metamorphic rocks, on the other hand, tend to be depleted in radioelements. Such depletion is actually part of the process that feeds the upper crust with relatively higher concentrations of radioelements [11]. In geothermal investigations, gamma-ray surveying is also useful for fracture identification. Fractures in the subsurface have previously been associated with elevated uranium concentrations due to the mobility of uranium in subsurface fluid circulation [12, 13]. In a bid to ascertain the geothermal potential in these quarries for possible energy generation, the subsurface radionuclides signatures from the quarries were utilized in estimating the total heat production and heat flow of the areas. The natural radiation from these granite bodies and other geological formation are other sources of environmental hazard [14]. Hence information on radiogenic heat production and heat flow within the subsurface is critical in the quest for geothermal energy exploration in these quarry sites. The knowledge of natural radioactivity in granite quarries is of great importance to determine the associated radiological hazards to those working in the quarries, those living in the neighborhood of the quarries, and the various buildings in which the granite would be used. This research aims to contribute to a better understanding of the natural radioactivity concentration, radiological health risk and radiogenic heat properties associated with the quarry sites, quarry products, workers and nearby residents of the quarry sites.

2. Methodology

2.1 Location and geology of study area

The study areas were located in the Central and Northern part of Ondo State, Nigeria and lies between latitudes $5^{\circ} 52'$ and $7^{\circ} 00'$ N and longitudes $4^{\circ} 23'$ and $5^{\circ} 54'$ E (Fig. 1). The geology of

this study area is of Precambrian rocks that are characteristic for the basement Complex of Nigeria [15, 16]. The major rock found within the area form part of the Proterozoic schist belts of Nigeria (Fig. 1). In terms of structural features, lithology and mineralization, the schist belts of Nigeria show considerably similarities to the Achaean Green Stone Belts. The terrain is flat with gently undulating topography. The sedimentary terrain of Ondo State falls within the eastern portion of the Dahomey Basin. The geologic sequence composed of the Nkporo Shale, Upper Coal Measures, Imo Shale Group, Coastal Plain Sands (Benin Formation) and Quarternary Coastal Alluvium (Fig. 1). The local geological mapping of the study area revealed that the area is underlain mainly by a rock unit, granite gneiss. The rocks are concealed in most areas and some outcrops are exposed around the study area. All the exposed outcrops observed have low fractures, indicating minor evidence of deformation. The megascopic minerals observed in this rock type include granite, quartz, feldspar and biotite which are used by the company for making other tiles etc. Generally, the sedimentary terrain of Ondo State falls within the eastern portion of the Dahomey Basin. The geologic sequence is composed of the Nkporo Shale, Upper Coal Measures, Imo Shale Group, Coastal Plain Sands (Benin Formation) and Quarternary Coastal Alluvium. The major rivers flow through the sedimentary rocks in deeply incised valleys aligned in a north-south direction. The locations are suspected to be characterized by solid mineral deposit as proposed by some studies [15, 16]. The topography of the area is gentle with few local outcrops in the northeastern and northwestern part.

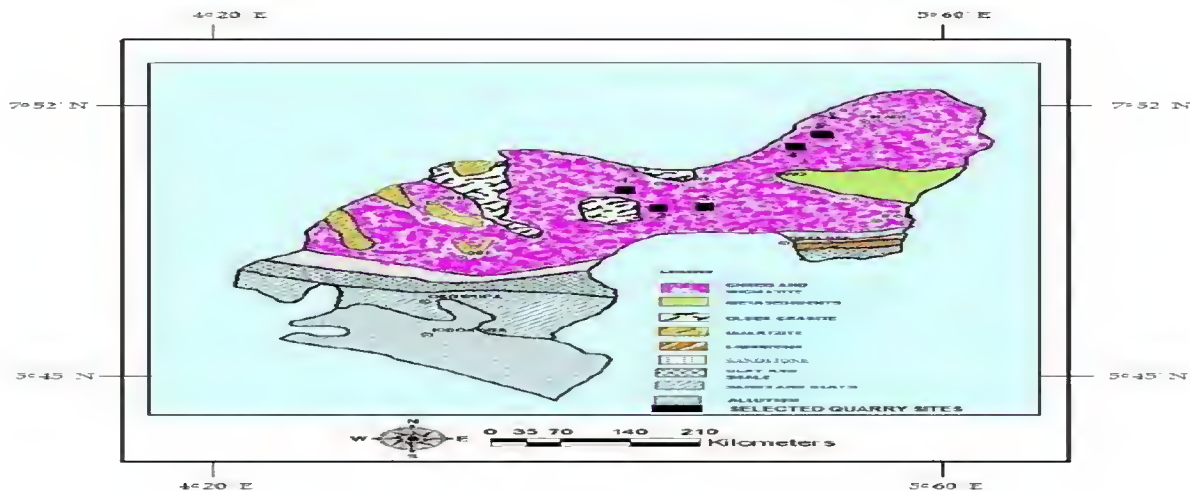


Fig 1: Geological Map of Ondo State Showing Location of the Different Quarries

2.2 Measurements Technique

Measurements were taken in five selected quarry sites in Ondo State: Sutol Quarry, Supare Akoko; Batista quarry, Ifon; Aslos quarry, Akure; Johnson quarry, Akure and Stoneworks quarry, Akure. Data was collected between January and February, 2020. A Gamma-ray spectrometer (Gamma Surveyor) was used to measure the values of the radioelements in the surveyed location. The instrument was placed on top of the rocks inside the quarry sites to take the reading on the screen of the instrument, but at location points where there was no rock, the instrument was held at a stable position and height to take the measurements. Also, outside the quarry sites, the instrument was held at a stable height and position in order to take the measurements. Measurements were made on traverses established across the study area. Measurements were taken at every 10 meters along the traverse, and the resultant concentrations of Potassium (^{40}K), Thorium (^{232}Th) and

Uranium (^{238}U) were recorded respectively alongside the geological coordinates (Longitude, Latitude and Universal Traverse Mercator). Once a traverse was completed, the next traverse was obtained by a 100 meters inter-traverse spacing. The measurement displayed on the screen with respect to (^{40}K), (^{232}Th) and (^{238}U) composition in the location. There are differences at each location using the Global Positioning System (GPS) which seems to be randomized values. The measurement of (^{232}Th) and (^{238}U) are in Parts per Million (PPM) and the (^{40}K) was measured in Percentage (%). The GPS was used to locate the geological, coordinates of the measured location.

2.3 Evaluation of radiological parameters

2.3.1 Conversion of radioelement concentration to specific activity

The mass concentration of uranium, thorium in parts per million (ppm) and potassium in % are converted to Bqkg^{-1} using (IAEA-TECDOC, 2003); 1% K in rock = 313 Bqkg^{-1} for ^{40}K ; 1 ppm U in rock = 12.35 Bqkg^{-1} for ^{238}U or ^{226}Ra and 1 ppm Th in rock = 4.06 Bqkg^{-1} for ^{232}Th . Contamination of the Earth's surface by man-made radionuclides is expressed by specific activity or activity per unit mass, (Bqkg^{-1}).

2.3.2 Absorbed dose rate

The activity concentration resulting from radionuclides were converted to absorbed dose rate in air by the relation [14]:

$$D(\text{nGyh}^{-1}) = 0.462C_u + 0.604C_{Th} + 0.0417C_k \quad (1)$$

Where D is the absorbed dose rate in nGyh^{-1} , C_u , C_{Th} and C_k are the activity concentration of ^{238}U , ^{232}Th and ^{40}K respectively. The conversion factors used to compute absorbed gamma dose rate (D) in air per unit activity concentration in (Bqkg^{-1}) samples are 0.462 nGyh^{-1} for ^{238}U , 0.604 nGyh^{-1} for ^{232}Th and 0.0417 nGyh^{-1} for ^{40}K [7, 17].

2.3.3 Annual effective dose equivalent

The annual effective dose equivalent received by human is estimated from absorbed dose rate by applying dose conversion coefficient from absorbed dose and occupancy factor which is defined as the level of human occupancy in an area in proximity with radiation source. The occupancy factor for outdoor is given as 20 % of 8760 hours in a year. Under these assumptions, the AEDE was calculated by the equation [8, 7, 18].

$$AEDE (\text{mSvy}^{-1}) = D(\text{nGyh}^{-1}) \times 8760 \times 0.7 \text{ SvGy}^{-1} \times 0.2 \times 10^{-6} \quad (2)$$

2.3.4 Hazard indices

External hazard index, H_{ex} , due to gamma radiation expected to be emitted externally from the building material was calculated using [8, 19].

$$H_{ex} = \frac{C_u}{370} + \frac{C_{Th}}{259} + \frac{C_k}{4810} (\text{Bqkg}^{-1}) \quad (3)$$

Internal hazard index, H_{in} , arises from inhalation of radon gas and its short lived decay progeny from the decay of ^{238}U . The internal exposure to ^{222}Rn gas is determined using [8].

$$H_{in} = \frac{C_u}{185} + \frac{C_{Th}}{259} + \frac{C_k}{4810} (\text{Bqkg}^{-1}) \quad (4)$$

Where C_u , C_{Th} , C_k are the specific activity (Bqkg^{-1}) of ^{238}U , ^{232}Th and ^{40}K respectively.

2.3.5 Alpha index (I_α)

Alpha index representative (I_α) is the evaluation of excess α -radiation ascribable to the radon inhalation coming from building materials. It is calculated with [8].

$$(I_{\alpha}) = \frac{C_u}{200} (Bqkg^{-1}) \quad (5)$$

Where C_U is the specific activity of concentration of ^{238}U .

2.3.6 Radiogenic heat production and heat flow estimation and implications

The calculated heat productions per sec in (ppm) are given in Table 3. These were estimated using the [20] relationship given as;

$$HP = 95.2 C(U) + 25.6 C(Th) + 0.000348 C(K) \quad (6)$$

Where HP is the quantity of heat produced due to the specific activity concentrations by weight $C(U)$, $C(Th)$ and $C(K)$ of Uranium, Thorium and Potassium in ppm respectively. On the other hand, heat flows from the quarry sites locations within the state were calculated using Turcotte and Schubert relationship [21] given as:

$$H_f = \frac{H_{RT}}{S} (Mm + Cr) \quad (7)$$

where H_f is the heat flow in (mWm^{-2}), H_{RT} is the total heat production from radioactive decay in the rock; $Mm + Cr$ is the mass of mantle plus crust given as 4×10^{24} kg and S is the total surface area of the earth given as 5.1×10^{14} m^2 . The heat flow computation is also presented in Table 3.

3. Results and Discussion

3.1 Activity concentration of natural radionuclides

The results of activity measurements of ^{238}U , ^{232}Th and ^{40}K for each quarry site are displayed in Table 1 in parts per million (ppm) and the corresponding conversion in Bqkg^{-1} . The activity concentration value varied from quarry to quarry both inside and outside the quarries. In Sutol quarry, the mean activity concentration value inside the quarry for ^{238}U , ^{232}Th and ^{40}K are (35.7, 107.25 and 1016.69) Bqkg^{-1} and for outside the quarry (24.8, 97.03, 992.49) Bqkg^{-1} respectively. In Batista quarry, the mean activity concentration value inside the quarry for ^{238}U , ^{232}Th and ^{40}K are (54.55, 101.36, and 1092.63) Bqkg^{-1} and (44.05, 84.68 and 941.35) Bqkg^{-1} for outside respectively. In Aslos quarry, the mean activity concentration value inside the quarry for ^{238}U , ^{232}Th and ^{40}K are (47.14, 81.5 and 1064.83) Bqkg^{-1} and for outside the quarry (39.15, 71.9 and 804.93) Bqkg^{-1} respectively. In Johnson quarry, the mean activity concentration value inside the quarry for ^{238}U , ^{232}Th and ^{40}K are (53.0, 106.81 and 1339.64) Bqkg^{-1} and for outside the quarry (30.67, 91.89 and 998.47) Bqkg^{-1} respectively. In Stonework quarry, the mean activity concentration value inside the quarry for ^{238}U , ^{232}Th and ^{40}K are (45.08, 78.16 and 1081.63) Bqkg^{-1} and for outside the quarry (40.14, 70.37 and 1061.33) Bqkg^{-1} respectively. Generally, ^{40}K contributed the highest activity concentration followed by ^{232}Th and ^{238}U .

3.2 Absorbed dose rate (nGyh^{-1})

The calculated absorbed gamma dose rate in air 1m above the ground surface for the study area ranged from 113.1 nGyh^{-1} in Stonework quarry to 144.86 nGyh^{-1} in Johnson quarry with a mean value of $125.80 \pm 12.99 \text{ nGyh}^{-1}$ inside the quarries and from 95.08 nGyh^{-1} in Aslos quarry to 111.45 nGyh^{-1} in Sutol quarry with a mean value of $106.78 \pm 7.02 \text{ nGyh}^{-1}$ outside the quarries in Table 2. The absorbed dose rate in air is highest in Johnson quarry inside and in Sutol quarry outside the quarries. The highest contribution to the absorbed dose rate in air comes from ^{40}K , followed by

^{232}Th and then ^{238}U in all the quarries. The absorbed dose rate in air in all the quarries is above the world average value of 60 nGyh^{-1} [14] and 84 nGyh^{-1} [22].

3.3 Annual effective dose equivalent (Aede)

The results of annual effective dose equivalent are presented in Table 2. It varied from an average value of 0.55 mSvy^{-1} in Stonework quarry to an average value of 0.71 mSvy^{-1} in Johnson quarry inside the quarries with a total mean of $0.62\pm0.06\text{ mSvy}^{-1}$ in all the quarries and from average value of 0.47 mSvy^{-1} in Aslos quarry to average value of 0.55 mSvy^{-1} in Sutol quarry outside the quarries with a mean total of $0.52\pm0.03\text{ mSvy}^{-1}$ in all the quarries. The mean AEDE in all the quarries is lower than the recommended limit of 1 mSvy^{-1} recommended for the members of the public [22, 23].

3.4 Estimation of risk assessment

The evaluated external risk (H_{ex}) ranged between a mean values of 0.65 in Stonework quarry to 0.83 in Johnson quarry with a mean value of 0.73 ± 0.08 inside the quarries. The evaluated external risk assessment ranged between an average values of 0.55 in Aslos quarry to 0.65 in Sutol quarry with an average value of 0.62 ± 0.04 outside the quarries. The estimated internal risk assessment (H_{in}) ranged between an average values of 0.77 in Stonework quarry to 0.98 in Johnson quarry with an average value of 0.85 ± 0.08 in all the quarries. The estimated average value of 0.66 in Aslos quarry to 0.76 in Batista quarry with a mean value of 0.71 ± 0.04 in all the quarries outside the quarries. These values in Table 2 do not exceed the acceptable limit of unity. This suggests that radiation hazard due to the exposure to natural radionuclides inside the quarries is negligible.

3.5 Alpha index (I_{α})

The estimated alpha index in Table 2 ranged between 0.18 in Sutol quarry to 0.27 in Batista quarry with a mean value of 0.24 ± 0.04 inside the quarries. The estimated alpha index ranged between 0.12 in Sutol quarry to 0.22 in Batista quarry with an average value of 0.18 ± 0.04 outside the quarries. (I_{α}) is lowest in Sutol quarry and highest in Batista both inside and outside the quarries. The alpha index in all the quarries is lower than the recommended exception level of 0.5 and upper limit of 1.0 in building materials as safety level [24, 25].

3.6 Radiogenic heat evaluation from the various quarries

Considering radionuclide concentrations, Uranium concentration is highest in the Johnson quarry (10.4 ppm) followed by Batista (9.0 ppm); Aslos (8.9 ppm); Stoneworks (8.2 ppm); and Sutol (6.2 ppm) respectively but on the average Batista (3.99 ppm) has the highest Uranium concentration followed by Aslos (3.52 ppm); Stoneworks (3.45 ppm); Johnson (3.39 ppm) and Sutol (2.43 ppm). The thorium plot (Figure 4) indicated that highest concentration of thorium falls within the Batista quarry (43.5 ppm) followed by Johnson (42.5 ppm); Aslos (37.5 ppm); Sutol (36.5 ppm) and Stone works (30.6 ppm). The potassium plot (Figure 4) shows highest concentration of potassium in Batista quarry (5.19%) followed by Johnson (5.16%); Stoneworks (4.93%); Sutol (4.84%) and Aslos (4.68%). The Minimum, Maximum and Average concentrations of Uranium, Thorium and Potassium for the different quarries are presented in (Table 3) respectively.

The Total Heat Production (THP) values estimated for all the quarries varied from 0.97 to $5.37\text{ }\mu\text{Wm}^{-3}$ thus making Johnson quarry the highest THP ($5.37\text{ }\mu\text{Wm}^{-3}$) followed by Aslos ($4.68\text{ }\mu\text{Wm}^{-3}$); Batista ($3.92\text{ }\mu\text{Wm}^{-3}$); Sutol ($3.91\text{ }\mu\text{Wm}^{-3}$) and Stoneworks ($3.72\text{ }\mu\text{Wm}^{-3}$). The heat production

value is on the high side which is an indication that the areas could be source of radiogenic heat and therefore needs further probing for possible geothermal potentials. On the other hand the heat flow estimation indicated Johnson quarry to have the highest heat flow value (42.12 mWm^{-2}) followed by Aslos (36.7 mWm^{-2}); Batista (30.77 mWm^{-2}); Sutol (30.65 mWm^{-2}) and Stoneworks (29.20 mWm^{-2}). From all indications, the rock samples and formation within the Johnson quarry are moderately high in radiogenic heat and contains minerals contributing to the respective heat production of the rocks and this could be a potential site for further probing for geothermal energy. This is also applicable to the Aslos quarry. The high Uranium and Thorium content in the rocks around these two quarries could be responsible for the high heat production and heat flow values observed in the area. Quarries with higher value concentrations of Uranium and Thorium coincide with that of having high heat production and heat flow and these are the Johnson and Aslos quarries.

In order to compare the gamma ray activity between the radioelements in the different quarries, the mean activity of each radioelement for each quarry from the spectrometric data acquired were estimated and the results presented as a bar chart (Figs. 2 to 5) and also variation of each radioelement with the radiogenic heat were presented as plots (Figs 6-10).

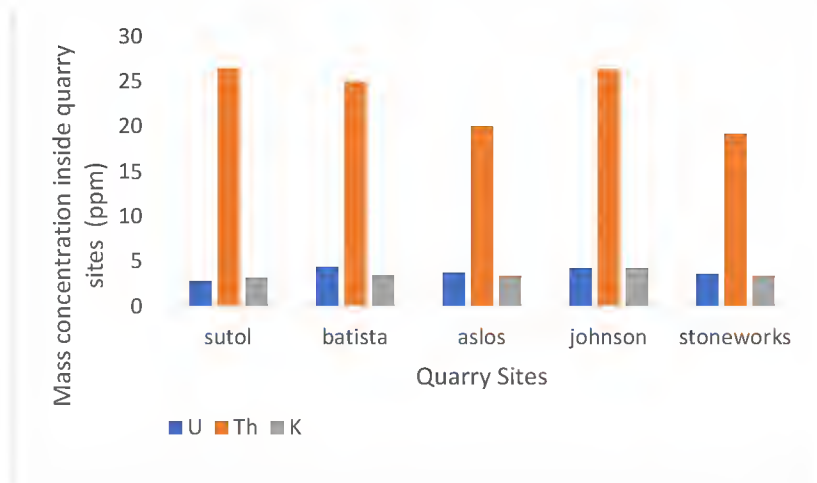


Fig: 2. Mass Concentration of Radionuclides (ppm) outside the quarries

Table 1: Mean Activity Concentration of Radionuclides Inside and Outside Different Quarries in Ondo State

Location	Inside						Outside					
Quarry sites	²³⁸ U		²³² Th		⁴⁰ K		²³⁸ U		²³² Th		⁴⁰ K	
	ppm	Bqkg ⁻¹	ppm	Bqkg ⁻¹	Ppm	Bqkg ⁻¹	ppm	Bqkg ⁻¹	ppm	Bqkg ⁻¹	ppm	Bqkg ⁻¹
Sutol	2.89	35.7	26.42	107.25	3.25	1015.69	2.01	24.8	26.42	107.25	3.25	3.17
Batista	4.42	54.55	24.97	101.36	3.49	1092.63	3.57	44.05	24.97	101.36	3.49	3.01
Aslos	3.82	47.14	20.08	81.50	3.40	1064.83	3.17	39.15	20.08	81.5	3.40	2.57
Johnson	4.29	53.0	26.31	106.81	4.28	1339.64	2.483s	30.67	26.31	106.81	4.28	3.19
Stonework	3.65	45.08	19.25	78.16	3.45	1080.63	3.25	40.14	19.25	78.16	3.45	3.39

Table 2: Radiological Parameters inside and outside the quarries

Location	Inside					Outside				
Quarry Sites	D(nGyh ⁻¹)	AEDE (mSvy ⁻¹)	I _a	H _{ex}	H _{in}	D(nGyh ⁻¹)	AEDE (mSvy ⁻¹)	I _a	H _{ex}	H _{in}
Sutol	123.63	0.61	0.18	0.72	0.82	111.45	0.55	0.12	0.65	0.72
Batista	131.99	0.65	0.27	0.77	0.91	110.75	0.54	0.22	0.64	0.76
Aslos	115.41	0.57	0.24	0.66	0.79	95.08	0.47	0.20	0.55	0.66
Johnson	144.86	0.71	0.27	0.83	0.98	111.31	0.55	0.15	0.65	0.73
Stonework	113.10	0.55	0.23	0.65	0.77	105.31	0.52	0.20	0.60	0.71
Mean	125.80	0.62	0.24	0.73	0.85	106.78	0.52	0.18	0.62	0.71
SD	12.10	0.06	0.03	0.08	0.09	7.02	0.03	0.04	0.04	0.04

Table 3: Radiogenic Heat Production and Heat Flow estimation data from the different quarries in Ondo State

Quarry sites	K (%)	U(ppm)	Th(ppm)	Northing	Easting	HP per sec			THP (μWm^{-3})	Heat flow (mWm^{-2})
						K	U	Th		
STONEWORKS QUARRY	3.75	2.5	20	803205	827908	0.35	0.65	1.42	2.43	19.04
	2.32	8.2	19.2	803205	827896	0.22	2.14	1.36	3.72	29.20
	2.79	5.9	15	803205	827884	0.26	1.54	1.07	2.87	22.50
	4.68	4.6	16.7	803202	827870	0.44	1.20	1.19	2.83	22.19
	4.54	0.5	18.7	803208	827860	0.43	0.13	1.33	1.89	14.80
	3.7	2.6	27.6	803205	822750	0.35	0.68	1.96	2.99	23.44
	4.11	3.8	19.8	803206	827840	0.39	0.99	1.41	2.79	21.86
	3.47	6.9	11.8	803203	827827	0.33	1.80	0.84	2.97	23.27
	3.69	0	20.3	803202	827814	0.35	0.00	1.44	1.79	14.04
	2.45	3	25.9	803205	827803	0.23	0.78	1.84	2.85	22.38
	3.12	0	25	803203	827789	0.29	0.00	1.78	2.07	16.24
	2.81	1	11	803204	827779	0.27	0.26	0.78	1.31	10.26
	3.27	3.1	12.3	803155	827913	0.31	0.81	0.87	1.99	15.62
	4.2	2.4	10.9	803153	827902	0.40	0.63	0.77	1.80	14.10
	2.92	6.3	19.5	803152	827892	0.28	1.64	1.38	3.31	25.93
	2.05	6.9	11.8	803151	827881	0.19	1.80	0.84	2.83	22.22
	2.54	1.1	18.6	803148	827868	0.24	0.29	1.32	1.85	14.49
	2.84	0	28.1	803145	827858	0.27	0.00	2.00	2.26	17.75
	2.05	6.4	13.3	803145	827847	0.19	1.67	0.94	2.81	22.03
	4.64	0	23.7	803143	827836	0.44	0.00	1.68	2.12	16.64
	3.39	2.1	15.4	803141	827824	0.32	0.55	1.09	1.96	15.39
	3.91	6	8.9	803140	827812	0.37	1.57	0.63	2.57	20.14
	4.93	6.6	14.9	803136	827801	0.47	1.72	1.06	3.25	25.47
	3.95	2.9	30.6	803134	827792	0.37	0.76	2.17	3.30	25.91
Minimum	2.05	0.00	8.90	803134.00	822750.00	0.19	0.00	0.63	1.31	10.26
Maximum	4.93	8.20	30.60	803208.00	827913.00	0.47	2.14	2.17	3.72	29.20
Average	3.42	3.45	18.29	803174.83	827635.25	0.32	0.90	1.30	2.52	19.79

Standard Deviation	0.85	2.64	6.09	30.60	1041.34	0.08	0.69	0.43	0.61	4.80
SUTOL QUARRY	4.41	3.5	36.3	793425	823665	0.42	0.91	2.58	3.91	30.65
	2.86	1.7	18.5	793421	823662	0.27	0.44	1.31	2.03	15.90
	2.64	0.7	21.7	793415	823665	0.25	0.18	1.54	1.97	15.48
	2.91	2.9	24.5	793413	823672	0.27	0.76	1.74	2.77	21.74
	2.18	0	27.9	793407	823682	0.21	0.00	1.98	2.19	17.15
	3.54	0.4	24.8	793403	822694	0.33	0.10	1.76	2.20	17.26
	4.84	1	23.2	793395	823700	0.46	0.26	1.65	2.37	18.56
	3.61	6.2	10.4	793393	823702	0.34	1.62	0.74	2.70	21.16
	2.08	4.8	24.2	793386	823708	0.20	1.25	1.72	3.17	24.85
	3.05	5.7	19.6	793379	823794	0.29	1.49	1.39	3.17	24.85
	2.76	4.9	31.8	793376	823712	0.26	1.28	2.26	3.80	29.79
	3.7	2.1	29.2	793279	823791	0.35	0.55	2.07	2.97	23.31
	4.24	0	35.7	793274	822800	0.40	0.00	2.54	2.94	23.03
	3.75	0.6	26.3	793268	823804	0.35	0.16	1.87	2.38	18.66
	3.53	3.9	21.3	793259	823804	0.33	1.02	1.51	2.86	22.47
	2.81	4	36.5	793254	823810	0.27	1.04	2.59	3.90	30.60
	2.85	4.9	18.1	793255	823820	0.27	1.28	1.29	2.83	22.23
	2.84	0	29.4	793245	823835	0.27	0.00	2.09	2.36	18.48
	3.26	0	31.4	793287	823816	0.31	0.00	2.23	2.54	19.90
	3.21	4.3	18.2	793302	823316	0.30	1.12	1.29	2.72	21.32
	2.79	0.6	33.9	793314	823313	0.26	0.16	2.41	2.83	22.18
	3.22	3.7	18.3	793315	823833	0.30	0.97	1.30	2.57	20.16
	2.74	0	18.7	793484	823847	0.26	0.00	1.33	1.59	12.45
Minimum	2.08	0.00	10.40	793245.00	822694.00	0.20	0.00	0.74	1.59	12.45
Maximum	4.84	6.20	36.50	793484.00	823847.00	0.46	1.62	2.59	3.91	30.65
Average	3.21	2.43	25.21	793345.61	823628.04	0.30	0.63	1.79	2.73	21.40
Standard Deviation	0.67	2.13	7.00	71.67	312.00	0.06	0.56	0.50	0.60	4.68
BATISTA QUARRY	3.12	4.3	31.9	802770	827886	0.29	1.12	2.27	3.68	28.88

	3.99	4.5	27.4	802767	827877	0.38	1.17	1.95	3.50	27.43
	3.81	6.4	13.4	802766	827868	0.36	1.67	0.95	2.98	23.39
	3.32	0	43.5	802761	827855	0.31	0.00	3.09	3.40	26.69
	4.67	2.2	36.8	802762	827848	0.44	0.57	2.61	3.63	28.46
	3.45	8.2	19.3	802767	827836	0.33	2.14	1.37	3.84	30.10
	2.43	7.2	22.4	802771	827821	0.23	1.88	1.59	3.70	29.02
	3.55	4.4	25.8	802767	827859	0.34	1.15	1.83	3.32	26.01
	5.19	4.9	16.7	802770	827808	0.49	1.28	1.19	2.96	23.18
	3.46	1.7	32.2	802774	827796	0.33	0.44	2.29	3.06	23.98
	2.24	0.2	23.2	802775	827786	0.21	0.05	1.65	1.91	14.99
	2.66	9	7	802772	827778	0.25	2.35	0.50	3.10	24.30
	4.24	3.1	38.2	802816	827906	0.40	0.81	2.71	3.92	30.77
	3.72	4.3	18.2	802819	827899	0.35	1.12	1.29	2.77	21.70
	2.18	6.7	10.3	802816	827887	0.21	1.75	0.73	2.69	21.07
	3.27	5.1	13.3	802814	827876	0.31	1.33	0.94	2.59	20.27
	3.23	6.6	14.9	802812	827868	0.31	1.72	1.06	3.09	24.21
	2.84	7.9	8.6	802811	827856	0.27	2.06	0.61	2.94	23.07
	3.89	0	28.3	802809	827845	0.37	0.00	2.01	2.38	18.64
	3.02	0	21.9	802811	827834	0.29	0.00	1.56	1.84	14.44
	3.18	0.1	27.9	802808	827823	0.30	0.03	1.98	2.31	18.10
	2.65	0.3	30.9	802808	827816	0.25	0.08	2.19	2.52	19.79
	2.15	4.8	16.6	802805	827808	0.20	1.25	1.18	2.64	20.67
	1.72	3.9	21.2	802809	827798	0.16	1.02	1.51	2.69	21.07
Minimum	1.72	0.00	7.00	802761.00	827778.00	0.16	0.00	0.50	1.84	14.44
Maximum	5.19	9.00	43.50	802819.00	827906.00	0.49	2.35	3.09	3.92	30.77
Average	3.25	3.99	22.91	802790.00	827843.08	0.31	1.04	1.63	2.98	23.34
Standard Deviation	0.83	2.89	9.66	22.35	36.64	0.08	0.75	0.69	0.58	4.51
						0.00	0.00	0.00	0.00	0.00
ASLOS QUARRY	4.02	7.8	20.9	802952	8027921	0.38	2.04	1.48	3.90	30.59
	2.32	1.4	15.5	802951	8027907	0.22	0.37	1.10	1.69	13.22
	3.14	3.9	21.3	802952	8027894	0.30	1.02	1.51	2.83	22.18

	3.15	2.2	16.9	802948	8027883	0.30	0.57	1.20	2.07	16.25
	4.68	1	3.8	802948	8027873	0.44	0.26	0.27	0.97	7.63
	3.69	4.1	3.4	802944	8027860	0.35	1.07	0.24	1.66	13.02
	2.21	8.1	17.7	802941	8027849	0.21	2.11	1.26	3.58	28.08
	4.24	0	37.5	802933	8027840	0.40	0.00	2.66	3.06	24.03
	3.05	2.7	21.4	802930	8027829	0.29	0.70	1.52	2.51	19.71
	3.52	0.5	18.7	802924	8027822	0.33	0.13	1.33	1.79	14.05
	3.83	7.1	34.7	803003	827922	0.36	1.85	2.46	4.68	36.70
	0.04	0.7	14.7	803004	827912	0.00	0.18	1.04	1.23	9.65
	0	1.2	10.2	803002	827900	0.00	0.31	0.72	1.04	8.14
	1.01	8.9	10.9	803000	827889	0.10	2.32	0.77	3.19	25.04
	0.43	6.5	11.1	802997	827878	0.04	1.70	0.79	2.53	19.81
	4.1	0	20.3	802993	827865	0.39	0.00	1.44	1.83	14.34
	3.85	1.5	7.9	802991	827854	0.36	0.39	0.56	1.32	10.33
	3.21	0.8	21.7	802988	827844	0.30	0.21	1.54	2.05	16.10
	3.23	6.2	25.6	802980	827832	0.31	1.62	1.82	3.74	29.35
	3.44	8.9	19.2	802980	827824	0.33	2.32	1.36	4.01	31.47
	4.41	4	35.1	802976	827813	0.42	1.04	2.49	3.95	31.01
	3.31	0	29.5	802970	827800	0.31	0.00	2.09	2.41	18.88
Minimum	0.00	0.00	3.40	802924.00	827800.00	0.00	0.00	0.24	0.97	7.63
Maximum	4.68	8.90	37.50	803004.00	8027921.00	0.44	2.32	2.66	4.68	36.70
Average	2.95	3.52	19.00	802968.50	4100591.41	0.28	0.92	1.35	2.55	19.98
Standard Deviation	1.39	3.17	9.42	26.69	3669463.20	0.13	0.83	0.67	1.09	8.54
JOHNSON QUARRY										
	4.67	3	24.5	803050	827926	0.44	0.78	1.74	2.96	23.25
	5.13	5.6	24.2	803052	827915	0.48	1.46	1.72	3.67	28.75
	4.02	4.2	24.3	80349	827904	0.38	1.10	1.73	3.20	25.11
	5.16	0	37.3	803046	827880	0.49	0.00	2.65	3.14	24.60
	4.23	2.1	7.8	803042	827892	0.40	0.55	0.55	1.50	11.78
	3.75	0	17.5	803042	827869	0.35	0.00	1.24	1.60	12.53
	4.78	0.5	24.8	803041	827856	0.45	0.13	1.76	2.34	18.38

	4.4	0	42.5	803040	827845	0.42	0.00	3.02	3.43	26.93
	4.24	9	36.9	803041	827836	0.40	2.35	2.62	5.37	42.12
	3.6	4.5	29.3	803043	827825	0.34	1.17	2.08	3.60	28.20
	3.64	0	31	803043	827814	0.34	0.00	2.20	2.55	19.96
	3.74	0.9	15.6	803041	827802	0.35	0.23	1.11	1.70	13.30
	2.51	1.9	20	803106	827926	0.24	0.50	1.42	2.15	16.89
	4.83	3.1	26	803101	827915	0.46	0.81	1.85	3.11	24.41
	3.95	3.3	21.4	803098	827903	0.37	0.86	1.52	2.75	21.60
	3.3	1.8	12.4	803096	827894	0.31	0.47	0.88	1.66	13.04
	3.44	0	34.3	803093	827884	0.33	0.00	2.44	2.76	21.65
	1.41	3.1	19.8	803091	827871	0.13	0.81	1.41	2.35	18.42
	2.96	3.1	26	803888	827863	0.28	0.81	1.85	2.94	23.02
	2.21	4.2	31.9	803086	827852	0.21	1.10	2.27	3.57	28.01
	3.16	10.4	22.1	8030884	827842	0.30	2.72	1.57	4.58	35.95
	3.05	4.7	22.7	803082	827833	0.29	1.23	1.61	3.13	24.53
	3.55	8.8	21.7	803079	827826	0.34	2.30	1.54	4.17	32.74
	3.91	7.1	13.3	803076	827812	0.37	1.85	0.94	3.17	24.84
Minimum	1.41	0.00	7.80	80349.00	827802.00	0.13	0.00	0.55	1.50	11.78
Maximum	5.16	10.40	42.50	8030884.00	827926.00	0.49	2.72	3.02	5.37	42.12
Average	3.74	3.39	24.47	1074146.25	827866.04	0.35	0.88	1.74	2.98	23.33
Standard Deviation	0.91	3.03	8.37	1489091.43	37.96	0.09	0.79	0.59	0.94	7.41

0=Below Detectable Limit (BDL)

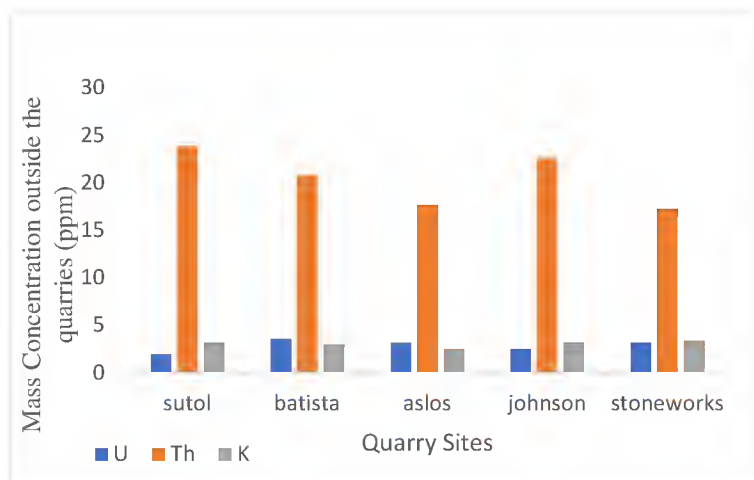


Fig: 3. Mass Concentration of Radionuclides (ppm) inside the quarries

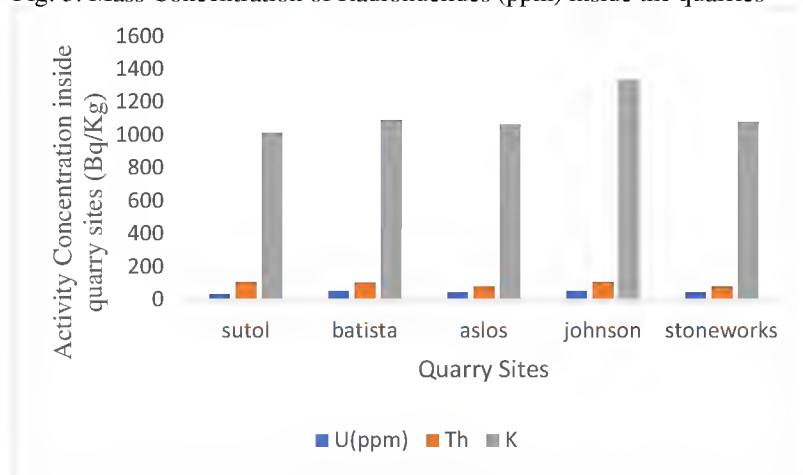


Fig 4. Activity Concentration of Radionuclides (Bq/kg) inside the quarries

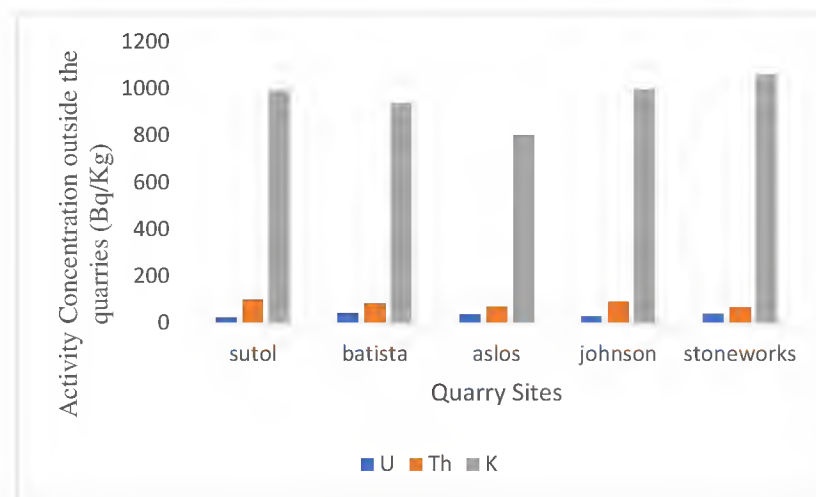


Fig 5. Activity Concentration of Radionuclides (Bq/kg) outside the quarries

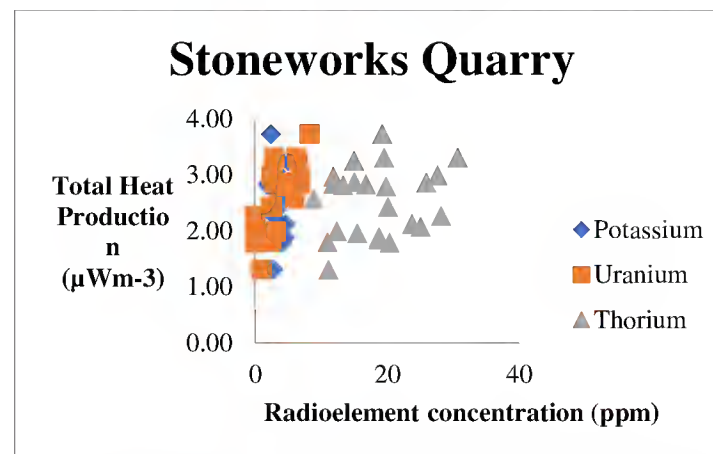


Fig 6. Heat production variation with radioelement concentration for Stoneworks quarry

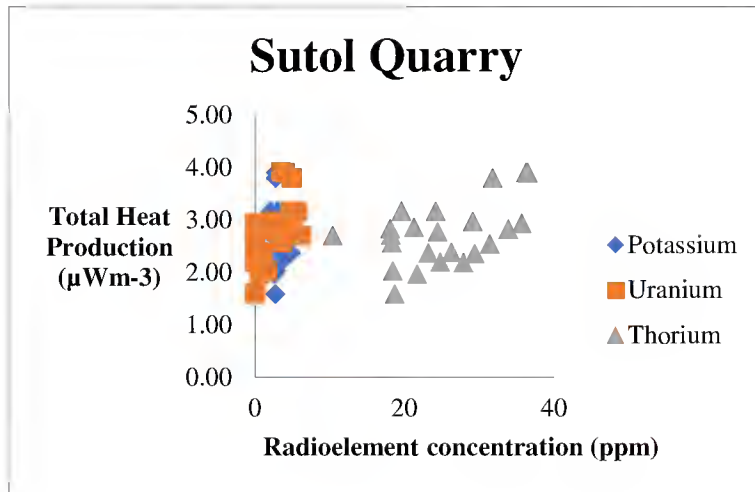


Fig 7. Heat production variation with radioelement concentration for Sutol quarry

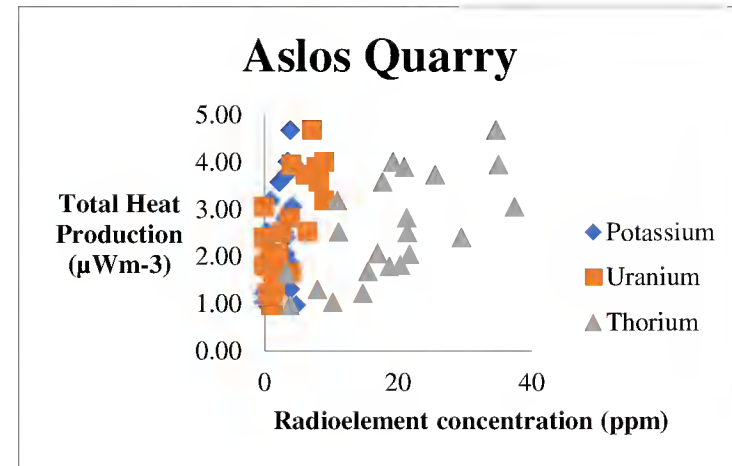


Fig 9. Plot of Heat production variation with radioelement concentration for Aslos quarry

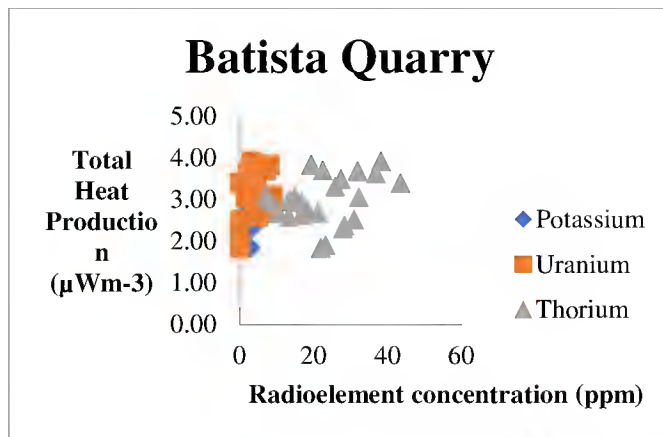


Fig 8. Heat production variation with radioelement concentration for Batista quarry

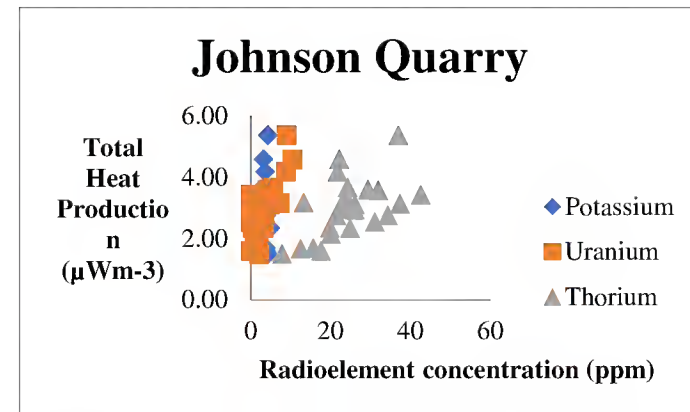


Fig 10. Heat production variation with radioelement concentration for Johnson quarry

4. Conclusion

The estimation of radiological risk, radiogenic heat production and heat flow for quarries in Ondo State have been deduced from ground radiometric data for common rocks types with the aim to be useful in geothermal modeling purposes. It could be shown that radiometric data could be useful for computing reliable values for heat flow of an area from numerical approach. The main conclusions derived from this work can be summarized as follows: Results from data analysis and interpretations have shown that the concentration of Thorium is higher compared to Uranium and Potassium which could be advantageous to agriculture practices in the different quarry sites. Also, this study has shown that the enrichment of Uranium, Thorium and Potassium concentrations in the rock samples reasonably satisfy the condition for the radioelements to be mined economically and further probe for geothermal energy exploration. This investigation has revealed that:

- i. The highest average concentrations of the radionuclides Uranium (^{238}U), Thorium (^{232}Th) and Potassium (^{40}K) in the different quarries are found in Batista quarry: 3.99 ppm, Sutol quarry: 25.21 ppm and Johnson: 3.74 % which are within the world average values.
- ii. Quarry of most promising Uranium mineralization is the Johnson quarry followed by Aslos quarry which could be an indication to consist of highly weathered minerals.
- iii. The elemental concentration of the radionuclides ^{238}U , ^{232}Th and ^{40}K in the different quarries are in the order (Th > U > K) (in ppm) which indicates preferential enrichment of Thorium to both Uranium and Potassium and in the order (K > Th > U) (in Bqkg⁻¹) for activity concentration.
- iv. The radiological hazard indices in all the quarries were found to be below unity. On the basis of low levels of natural radioactivity, the study areas can be considered as a less natural background radiation hazard area. The radioactivity of the rocks of the study area are therefore not harmful to human beings and the environment. It is concluded that the activity of the rocks of the study area has no harmful radiation effects to people and environment.

References

- [1] IAEA, (2003). IAEA-TECDOC-1363. Guidelines for Radioelement Mapping Using Gamma Ray Spectrometry Data. IAEA, Vienna.
- [2] Killeen, P. (1979). Gamma ray spectrometric methods in uranium exploration. Application and interpretation. *Geophys. Geochem. Search Met. Ores* 31: 163–230.
- [3] Bristow, C. and Williamson, B. (1998). Spectral gamma-ray logs: Core to log calibration, facies analysis and correlation problems in the Southern North Sea. *Geol. Soc. Lond. Spec. Publ.* 136: 1–7.
- [4] Rybach, L., Schwarz, G.F. (1995). Ground gamma radiation maps: Processing of airborne, laboratory, and *in situ* spectrometry data. *First Break*, 13: 97–104.
- [5] Ray, L., Roy, S., Srinivasan, R. (2008). High Radiogenic Heat Production in the Kerala Khondalite Block, Southern Granulite Province, India. *Int. J. Earth Sci.* 97: 257–267.
- [6] IAEA, (2003). Extent of environmental contamination by naturally occurring radioactive material and technological options for mitigation. Technical report series. No 419.
- [7] Supitha C., Chutima, K. Shinji, T. Napakans, S. Karnwalee, P. and Chanis, P. (2011). Terrestrial Gamma Radiation in Phuket Island, Thailand. *Engineering Journal.* 15(4): 65-72. doi:10.4186/ej.2011.15.4.65.
- [8] Ajayi, O.S., Faromika, O.P. Lawal, J.I. (2019). Estimation of natural radioactivity and radiological risk in granite from major quarries in Osun state Nigeria. *Int. J. of adv. research sci., engineering and techno.* 6(7): 1962-1970.
- [9] Ministry of Energy, British Columbia, (2014). Common rock types.
- [10] McCay, A., Harley, T. Younger, P. Sanderson, D. and Cresswell, A. (2014). Gamma-ray spectrometry in geothermal exploration: state of the art techniques. *Energies*, 7 (8): 4757-4780. ISSN pp 1996-1073
- [11] Kumar, P.S. and Reddy, G. (2004). Radioelements and heat production of an exposed Archaean crustal cross-section, Dharwar craton, south India. *Earth Planet. Sci. Lett.* 224: 309–324.
- [12] Quinn, T., Suzuki, N.I.M. Takagim, S. (1989). Mineralogy evaluation in a geothermal well using statistical probabilistic log evaluation techniques. *Geotherm. Resour. Counc. Trans.* 13: 277–287.
- [13] Younger, P., Manning, D. (2010). Hyper-permeable granite: Lessons from test-pumping in the Eastgate Geothermal Borehole, Weardale, UK. *Q. J. Eng. Geol. Hydrogeol.*, 43: 5–10.
- [14] UNSCEAR, (2000). Sources and Effects of Ionizing Radiation. Report to the general assembly with Scientific Annexes. United Nations, New York.
- [15] Elueze, A.A., (1986). Vertical Components of Ground Magnetic Studies of Ilesha area, Southwest Nigeria: Geological Survey of Nigeria
- [16] Rahaman, M.A., (1976). A Review of the Basement Geology of Southwestern Nigeria; Elizabeth Publishing Co. pp 41-58
- [17] Joel, E.S., Maxwell, O. Adewoyin, O.O. Olawole, O.C. Arijaje, T.E., Embong, S. and Saeed, M.A. (2019). Investigation of natural environment radioactivity concentration in soil of coastal area of Ado-Odo/Ota, Nigeria and its radiological implications. *Scientific Reports*. 9: 4219.
- [18] Ibrahim, M.S., Atta E.R. and Zakaria, K.M. (2014). Assessment of natural radioactivity of some quarries raw materials in El-Minya Governorate, Egypt. *Arab J. of natural science and application.* 47(1): 208-216.
- [19] Walley El-Dine, El-Shershaby, A. Ahmed, F. Abdel-Haleem, A.S. (2001). Measurement of radioactivity and radon exhalation rate in different kinds of marbles and granites. *Appl. Rad. and Iso.* 55: 853-860.
- [20] Rybach, L., (1988). Determination of heat production rate. In: Haenel, R., Rybach, L., Stegena, L. (Eds.), *Handbook of Terrestrial Heat-Flow Density Determination*. Dordrecht: Kluwer Academic Publishers. Dordrecht (1988), pp. 125–142.
- [21] Turcotte, D.L., Schubert, G. (2002). *Geodynamics* 2nd Edition. Cambridge University Press, Cambridge. Pp 456.
- [22] UNSCEAR, (2008). Sources and effects of Ionizing Radiation. Report to the General Assembly with Scientific Annexes. Vol 1, United State, New York.
- [23] ICRP, (2012). Compendium of Dose Coefficients Based on ICRP Publication 60. *Annals of the ICRP*. ICRP. 41 (1).
- [24] ICRP, (1994). Protection against Rn-222 at home and at work. ICRP Publication 65. *Annals of the ICRP*, 23, 1-38.
- [25] EC (European Commission), (1990). Commission recommendation 90/143/Euratom of 21 February, 1990 on the protection of the public against indoor exposure to radon. Official J L-80 of 27/03/90. Brussels